Photoinduced Energy/Electron Transfer within Single-Chain Nanoparticles

Masanori Nagao, Kai Mundsinger, and Christopher Barner-Kowollik**

Abstract: We demonstrate that single-chain nanoparticles (SCNPs) – compact covalently folded single polymer chains – can increase photocatalytic performance of an embedded catalytic center, compared to the comparable catalytic system in free solution. In particular, we demonstrate that the degree of compaction allows to finely tailor the catalytic activity, thus evidencing that molecular confinement is a key factor in controlling photocatalysis. Specifically, we decorate a linear parent polymer with both photoreactive chalcone moieties as well as $Ru(bpy)_3$ catalytic centers. We initially construct a SCNP via a photosensitized [2+2] cycloaddition at 510 nm and demonstrate that the SCNP formation is substantially more efficient when the $Ru(bpy)_3$ units are part of the polymer chain instead of as free molecules in solution. Subsequently, we employ the same $Ru(bpy)_3$ units as photocatalysts in a model reaction employing pyrene units as charge transfer moieties. We establish that the photocatalytic activity increases as the polymer becomes more compact, reaching peak efficiency, followed by a subsequent decline as the SCNP becomes too compact. Thus, we identify a goldilocks regime of catalyst confinement via SCNP compaction for use in photocatalysis.

[*] Dr. M. Nagao
Department of Chemical Engineering
Kyushu University
744 Motooka Nishi-ku, Fukuoka (Japan)
E-mail: nagaom@chem-eng.kyushu-u.ac.jp

Dr. M. Nagao, Dr. K. Mundsinger, Prof. C. Barner-Kowollik
School of Chemistry and Physics
Queensland University of Technology (QUT)
2 George Street,
Brisbane QLD 4000 (Australia)
and
Centre for Materials Science
Queensland University of Technology (QUT)
2 George Street
Brisbane QLD 4000 (Australia)
E-mail: christopher.barnerkowollik@qut.edu.au

Prof. C. Barner-Kowollik
Institute of Nanotechnology (INT)
Karlsruhe Institute of Technology (KIT)
Hermann-von-Helmholtz-Platz 1, 76344 Eggenstein-Leopoldshafen (Germany)

Prof. C. Barner-Kowollik
Institute of Functional Interfaces (IFG)
Karlsruhe Institute of Technology (KIT)
Hermann-von-Helmholtz-Platz 1, 76344 Eggenstein-Leopoldshafen (Germany)

Introduction

Biomacromolecules such as DNA and proteins feature precise structures, based on defined monomer sequences resulting in distinct geometries. These features allow for a specific spatial arrangement of functional groups leading them to execute molecular functions in a highly effective fashion. Encouraged by the superior design of nanomaterials in nature, polymer chemists have aimed at developing precision synthetic polymers with controlled polymer length, monomer sequence, and conformation.[1] In particular, the control of polymer conformation is rich with opportunities, because the exact folded structure of a protein is critical for their function (e.g., catalytic activity of enzymes). Single-chain nanoparticles (SCNPs) are a class of intramolecularly cross-linked synthetic polymers resulting in compact, folded structures.[2] The use of SCNPs in catalysis has been explored in several studies and continues to be an active and expanding field of research as recently highlighted by us.[3,4]

Perhaps one of the most well-known photoreaction systems in nature is photosynthesis, making use of specific biomacromolecules. This system involves a large protein complex (termed Photosystem II), in which multiple chlorophyll molecules are arranged at a distance of around 1 to 3 nm,[5] enabling efficient energy transfer from the light-absorbing chlorophyll molecules to the reactive entities. Clearly, this confinement of reactive functional groups on the nanometer length scale is critical and thus confinement of the catalytic moieties within single polymer chains provides an advantage for increasing the effectiveness of photoinduced reactions.[6] Previously, we reported several systems where a photochemical process benefitted from macromolecular confinement.[7] For example, the [2+2] photodimerization of styrylpyrene within single polymer chains was substantially accelerated compared to comparable free solution experiments, enabling the facile preparation of SCNPs.[7a] While the above examples demonstrate advantages of conducting photochemical processes within confined environments, to date there is no quantitative study of macromolecular confinement effects on photoinduced energy/electron transfer (PET) exploiting synthetic polymers.

Herein, we close this critical gap and demonstrate increased PET efficiencies when performed in a confined

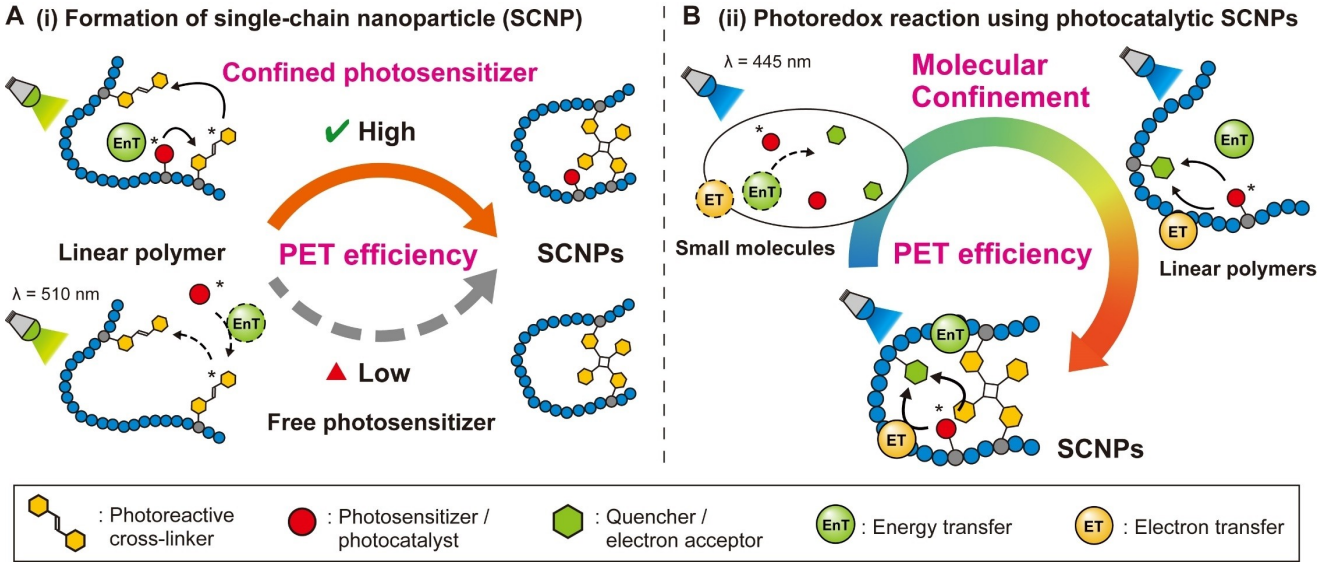

Figure 1. Schematic illustration of the current study. **(A)** Formation of single-chain nanoparticles (SCNPs) through photoinduced energy transfer (PET) from a photosensitizer to a cross-linker. **(B)** Photoredox reaction involving photoinduced energy transfer and electron transfer (PET) from a photosensitizer to a quencher.

polymer bound environment. First, we discuss the intramolecular photosensitization based on quantum yields. Subsequently, we investigate the effects of polymer folding on photocatalytic reactions within the single polymer chains. We exploit a photoreactive metal complex twice: Initially to aid construction of our SCNP system as a photosensitizer and subsequently to serve as a photocatalytic entity within the constructed SCNP environment (refer to Figure 1).

Results and Discussion

Formation of SCNPs via PET

The polymer at the core of our system is comprised of methyl methacrylate (MMA) and pyrene-chalcone methacrylate (PyChMA), able to undergo an intramolecular [2+2] photocycloadditon under irradiation with visible light (**P1** in Figure 2A).[7a,8] A statistical copolymer with a PyCh content of 11.5 mol % was obtained by reversible addition-fragmentation chain transfer (RAFT) polymerization (Table 1 and S1). The absorbance spectrum of **P1** solution in THF:acetonitrile (ACN) (1:2, vol:vol) displays the typical features of the PyCh unit (Figure S11 and S22A). We initially investigated the ability of **P1** to form SCNPs under visible light irradiation. After LED irradiation at $\lambda_{max}=$ 517 nm of a **P1** solution under the exclusion of oxygen, the absorbance bands of PyCh at 390 and 415 nm decreased along with the appearance of two new distinct bands at 335 nm and 353 nm (Figure S22A). These spectral changes are indicative of the progressing [2+2] cycloaddition of the PyCh units. Despite our previous work demonstrating no photoreactivity of the PyCh reaction above 500 nm,[8] we were able to efficiently form dimers using an LED with its emission centred at 517 nm. We hypothesize the weak blue emission tail of the LED is sufficient to efficiently progress the reaction (Figure S1). The rate of PyCh dimerization is oxygen dependent, with faster rates observed in deoxygenated solutions (Figure S22D). The decreased reaction rate in the presence of oxygen suggests that the photocycloadditon of PyCh proceeds via a triplet state. Size exclusion chromatography (SEC) analysis of **P1** after LED irradiation showed the elution volume shifted to larger volumes compared to **P1** (Figure S23). The shift in elution volume

Table 1: Properties of the employed polymer systems after cross-linking of the linear parent polymers into SCNPs.[a]

Compounds	M_n before irradiation/ g mol^{-1}[b]	M_n after irradiation/ g mol^{-1}[b]	PyCh unit ratio in polymer/mol %	PyCh/ μM[c]	Ru complex/ μM[c]	Φ
P1	10,800	9,400	11.5	20	0	n.d.
P1 + **Ru-(bpy)$_3$**	10,800	9,500	11.5	20	11	0.013 ± 0.003
P2	9,100	8,000	7.7	15	12	0.16 ± 0.02

[a] Wavelength of laser irradiation was 510 nm. The solvent mixture THF: acetonitrile = 1: 2 (vol:vol). [b] Molecular weights were determined by SEC analysis (THF, linear PMMA calibrants). [c] Concentrations of the PyCh and Ru complex were calculated via the molar absorption coefficient of PyCh unit and Ru complex (detailed calculations are shown in Table S6).

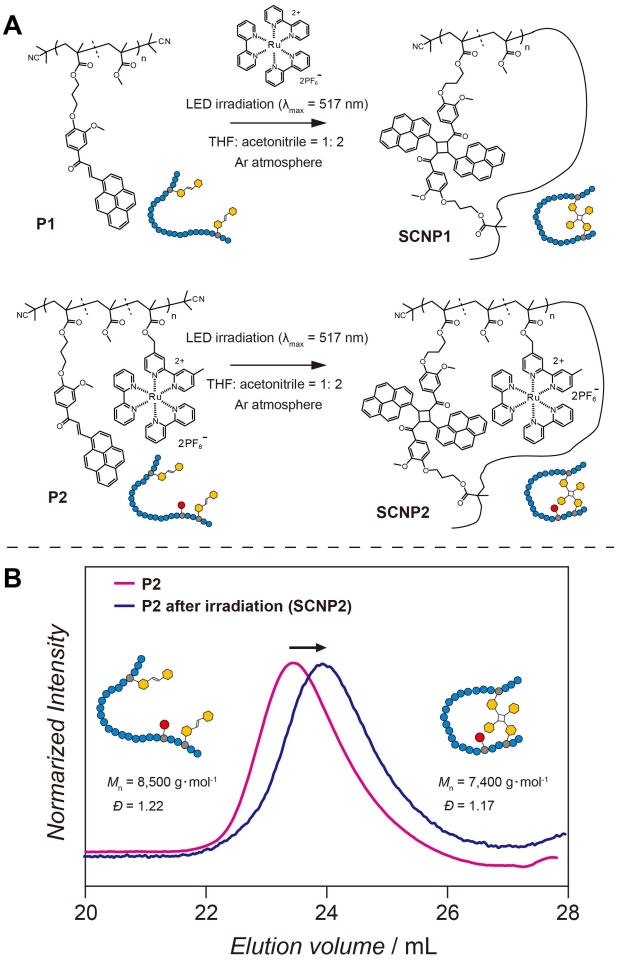

Figure 2. **(A)** Intramolecular crosslinking reaction of **P1** and **P2** through [2+2] cycloaddition of pyrene-chalcone under LED irradiation at $\lambda_{max}=517$ nm. The intramolecularly crosslinked **P1** and **P2** are denoted as **SCNP1** and **SCNP2**. **(B)** Size exclusion chromatography (SEC) traces in THF for **P2** before (magenta) and after (purple) LED irradiation at $\lambda_{max}=517$ nm, respectively.

demonstrates the successful formation of **SCNP1**. Hydrodynamic volumes of **P1** (V_H) were calculated using the hydrodynamic radius (r_H) observed in SEC (Table S2). Upon SCNP compaction, the hydrodynamic volume of **SCNP1** decreased by 20 % compared to **P1** (Table S2).

Subsequently, the effect of a photosensitizer on the PyCh reaction was investigated using tris(2,2'-bipyridyl) ruthenium (II) ($Ru(bpy)_3^{2+}$), featuring a broad absorption in the visible light region, with its maximum at 455 nm (Figure S7).[9] Under deoxygenated conditions, the presence of $Ru(bpy)_3^{2+}$ in the **P1** solution significantly accelerated the reaction rate (Figure S22B). The acceleration effect was not observed in the presence of oxygen. LED irradiation of **P1** in the presence of $Ru(bpy)_3^{2+}$ led to a shift to larger elution volumes compared to **P1**, with a molar mass distribution nearly identical to **SCNP1** when folded without the presence of the photosensitizer (Figure S23). The shift in elution volume indicates the successful formation of **SCNP1** in the presence of the photosensitizer without any effect on the polymer structure.

For photochemical sensitization to proceed efficiently, (photo)excited molecules (or units) must encounter a reactive partner within their excited lifetime. Both the excited-state lifetime and molecular diffusion rate are critical factors affecting photochemical efficiency. Therefore, co-locating the photosensitizer and PyCh units within the same polymer should significantly enhance the energy transfer efficiency due to the higher local concentration compared to a system using a photosensitizer in free solution. To test this hypothesis, the ruthenium bipyridyl complex was introduced into the parent polymer containing PyCh units by copolymerization of $Ru(bpy)_2$dmbpy methacrylate (**P2** in Figure 2). The resulting folding rate of **P2** was significantly higher than that of the mixture of **P1** and free $Ru(bpy)_3Cl_2$ (Figure S22C) at an identical concentration of the ruthenium species. Moreover, the PyCh reaction of **P2** proceeded at a faster rate than the free solution system even in the presence of oxygen, demonstrating that the intramolecular photosensitization exceeds the oxygen diffusion rate in the reaction system (Figure S22F).

To quantify the effect of macromolecular confinement of the photosensitizer on PET, we analyzed the reaction kinetics using a monochromatic tunable pulsed laser system.[7e] Our laser system emits light with a much narrower bandwidth (1 ± 0.3 nm) than an LED and allows to precisely control the number of photons deposited into the reaction system. The absorbance spectra of the polymer solutions were monitored in real time during laser irradiation (Figure 3). Laser irradiation of **P1** (deoxygenated solution) at 510 nm (6 mJ s^{-1}) did not result in any changes in the absorbance spectrum, consistent with our previous report (Figure 3A).[8] Irradiation of **P1** in the presence of $Ru(bpy)_3^{2+}$ slightly decreased the absorbance bands of PyCh (390 and 415 nm, Figure 3B), indicating that the addition of photosensitizer enabled the [2+2] cycloaddition of **P1** via PET. As PyCh itself exhibits no significant absorbance at 510 nm, we conclude that the reaction proceeds due to energy transfer from $Ru(bpy)_3^{2+}$ to PyCh. The polymer carrying the Ru complex (**P2**) showed the fastest decrease in the absorbance peaks even at a threefold lower laser power (2 mJ s^{-1}), demonstrating significantly higher PET efficiency in the intramolecular system than the free photosensitizer (Figure 3C).

Quantum yields for each system were calculated based on the number of photons deposited and the molar absorption coefficient at the corresponding wavelength (Figure 3D, and Table 1).[7e] The quantum yield (Φ) of **P2** folding was 0.16, which was tenfold higher than that of the **P1** and the free $Ru(bpy)_3^{2+}$ system ($\Phi=0.013$). These quantum yields describe the net reaction and encompass multiple reaction steps, including intersystem crossing of the Ru complex, energy transfer from the Ru complex to PyCh unit, and [2+2] cycloaddition between two PyCh units. The PyCh content in **P2** was 7.7 mol %, lower than that of **P1** (11.5 mol %), which would typically be less favorable for intramolecular [2+2] cycloaddition due to the increased distance between reaction partners.[7a] Nevertheless, the

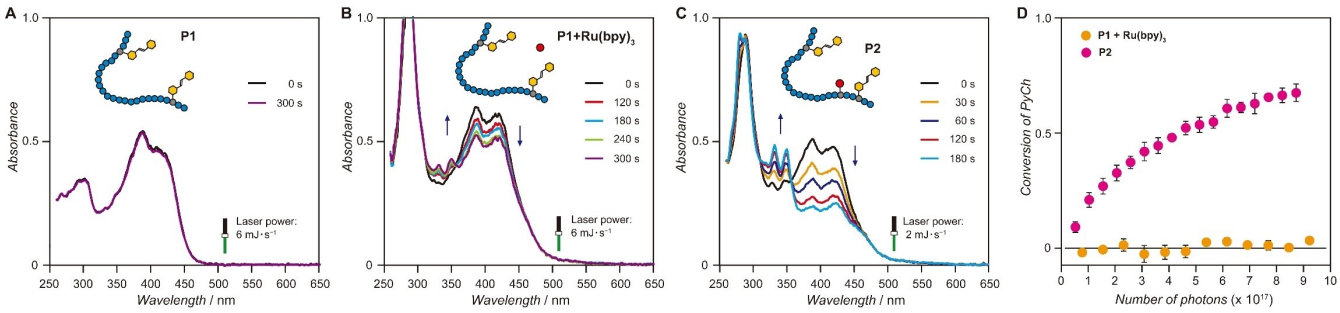

Figure 3. Real-time UV/Vis spectra of the polymer solution of **(A) P1** (0.023 g L^{-1}; 20 μM of PyCh unit), **(B) P1** (0.023 g L^{-1}; 20 μM of PyCh unit) with $Ru(bpy)_3$ (11 μM), and **(C) P2** (0.039 g L^{-1}; 15 μM of PyCh unit) upon laser irradiation at λ = 510 nm in THF:ACN (1:2, vol:vol). The laser power was 6 mJ s^{-1} for **(A)** and **(B)**, and 2 mJ s^{-1} for **(C)**. **(D)** Conversion of the pyrene-chalcone unit in the polymer structures vs number of deposited photons. Orange and magenta plots represent the **P1** with $Ru(bpy)_3$ and **P2** systems, respectively.

quantum yield of **P2** exceeds that of the free photosensitizer system, indicating that the energy transfer from the Ru complex to PyCh unit is significantly enhanced by the confinement of the Ru complex within the polymer. Notably, even at a high concentration (4 g L^{-1}, one order of magnitude greater than typical SCNP folding conditions), the SCNP originating from **P2** was obtained without the formation of intermolecularly cross-linked structures (Figure 2B) further evidencing the increased rates of the intramolecular reaction over intermolecular reactions. In summary, the incorporation of the photosensitizer into the chain polymer structure allowed the facile preparation of SCNPs more efficiently via visible-light induced [2+2] photocycloaddition.

SCNP-driven Photocatalysis

We subsequently applied the concept of molecular confinement via SCNPs to a photocatalytic reaction (refer to Figure 1B and Scheme 1) using our synthesized polymer system. As a model reaction, we selected photoredox reactions using pyrene and the Ru complex.[10a,11a] Several studies have explored the reaction mechanism and clarified that it is highly dependent on the chemical species in the system, such as the types of photosensitizer, electron donor, and quencher.[10] Herein, we discuss the reaction mechanism involving the Ru bipyridyl complex, DIPEA, and pyrene.[10d] The reaction follows five key steps; (i) the Ru complex is excited, and immediately undergoes intersystem crossing; (ii) pyrene is excited via triplet energy transfer from the Ru complex; (iii) the excited pyrene is quenched by the one-electron-reduced species of the Ru complex (e.g., $Ru(bpy)_3^{+}$), forming a pyrene radical anion ($Py^{\bullet -}$); (iv) the pyrene radical anion abstracts a halogen from the substrate; and (v) the radical species formed from the substrate is immediately trapped by *N*-methylpyrrole (Figure 5A). Herein, $Ru(bpy)_3^{2+}$ acts as a photocatalyst by both exciting pyrene and donating an electron to pyrene. We propose that the introduction of pyrene and the Ru complex into the SCNP structures enhances the PET process in step (ii) and (iii), leading to higher conversions under otherwise identical conditions. Control experiments using **SCNP1** demonstrate the necessity of $Ru(bpy)_3^{2+}$ for driving the reaction forward (Table 2).

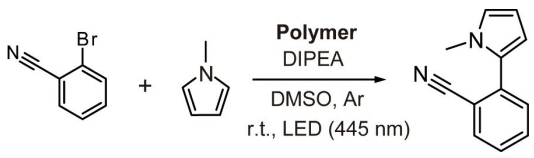

Scheme 1. Photoredox reaction employed to assess the efficacy of the polymer and SCNP catalytic reaction system.

Based on our initial assumption, we expected that the twin-pyrene units in the crosslinked PyCh-dimer of **SCNP2** would effectively trigger the photocatalytic reaction with the incorporated Ru complex. However, **SCNP2** exhibited a significantly lower reaction conversion compared to the other polymers discussed later (Table 2). We hypothesize that the steric constraint within the polymer chain rather than the cyclobutane motif effectively increases the distance between pyrene and Ru moieties causing the sluggish behavior. Our hypothesis was supported by a control experiment using a PyCh-dimer (compound **7** in the SI), demonstrating a reaction conversion similar to that of pyrene (Table S10). Based on these findings, we theorized that polymers containing free pyrene units after folding would overcome this limitation.

A series of polymers containing additional pyrene units was synthesized (**P3-CL2, -CL7**, and **-CL11** in Figure 4A). These polymers were designed to contain both pyrene units and Ru complex in the same ratios (2 mol % each), with varying PyCh cross-linker ratio of 2, 7, and 11 mol %, respectively. We investigated the consumption of the monomers via NMR spectroscopy to ensure the random nature of our copolymers. All monomers were consumed at the same rate during the polymerization, indicating a random distribution of monomers (Figure S21). The polymers were folded into SCNPs via LED irradiation at 517 nm (**SCNP3-CL2**, **-CL7**, and **-CL11** in Figure 4A and Table 2). Absorbance spectra and SEC analysis confirmed the formation of SCNPs without observable intermolecular cross-

Table 2: Conversion of photoredox reaction with synthesized polymers or free pyrene and $Ru(bpy)_3$.[a]

Catalyst	PyCh unit/mol %[b]	Pyrene unit/mol %[b]	$Ru(bpy)_2$dmbpy unit/mol %[b]	*Time*/min	*Conversion*/%[c]
SCNP1[d]	11.5	–	–	60	0
SCNP1 + $Ru(bpy)_3$[d]	11.5	–	–	30	5
				60	12
SCNP2	7.7	0	3.3	30	2.5 ± 0.5
				60	5.0 ± 0.2
SCNP3-CL2	2.3	2.6	2.5	30	17.7 ± 0.5
				60	24.3 ± 0.5[e]
SCNP3-CL7	6.6	2.0	2.2	30	16.0 ± 0.0
				60	25.0 ± 0.0
SCNP3-CL11	11.3	2.2	2.2	30	15.0 ± 0.8
				60	22.0 ± 1.6
P4	0	2.5	3.0	30	15.7 ± 0.9
				60	19.7 ± 1.2
Pyrene + $Ru(bpy)_3$	–	–	–	30	12.3 ± 1.2
				60	20.0 ± 2.2

[a] The reaction solution was prepared using DMSO-d_6 with 2-bromobenzonitrile (80 mM), *N*-methylpyrrole (0.8 M), and DIPEA (100 mM). The concentration of each polymer was set so that [Ru] was close to 1 mM. The solution was purged with argon for 10 min. The wavelength maximum of LED irradiation was 445 nm. [b] Unit ratios in the polymer structure were determined by ^{1}H NMR spectroscopy. [c] Conversions after 30 min irradiation was determined by ^{1}H NMR spectroscopy. Detailed calculations are shown in Figure S25. The experiments were triplicated. [d] The amount of **SCNP1** was close to 5 mg. [e] Conversion was 0% in the absence of DIPEA.

linking (Table S3, Figure S24 and S25). Notably, the shift observed in SEC traces increased with the cross-linking ratio (Figure S25). Upon folding, **SCNP3-CL2** exhibited close to 5% compaction, **SCNP3-CL7** showed ca. 13% compaction and **SCNP3-CL211** was compacted by approx. 22% compared to their respective parent polymers (Table S4). These values suggest a linear correlation with the cross-linker content of the polymers, leading to more compact structures of **SCNP3 s** with higher cross-linker content (Figure 4B).

A linear polymer containing pyrene units and Ru complex, yet without PyCh units, was also prepared as a non-crosslinked reference system (**P4** in Figure 4 and Table 2). The reaction solution was prepared using the photocatalytic polymers, 2-bromobenzonitrile as the substrate, *N*-methylpyrrole as the trapping agent, and DIPEA as the electron donor in DMSO-d_6. After LED irradiation at 445 nm, the consumption of 2-bromobenzonitrile was followed via ^{1}H NMR spectroscopy (Figure 5B). In the absence of DI PEA, no reaction progress was observed, confirming that DI PEA acts as the electron donor in the reaction (Table 2). The reaction conversion was calculated based on the integral values of the proton resonances at 6.16, 6.34, 6.97, and 7.94 ppm (for details refer to Figure S30).[10d] Although the reaction conditions were optimized (Table S11), the substrate conversion became saturated with continuous light irradiation (Figure S31). Absorbance spectra of the reaction solution after irradiation indicated photodegradation of the Ru complex during the reaction, which was not observed in the absence of DI PEA (Figure S32). Furthermore, the conversion decreased under conditions with an increasing amount of DI PEA (Table S11), suggesting that the degradation occurs in the reduced Ru species, which is relatively unstable under irradiation.[11] Appearance of peaks at large elution volumes during SEC analysis after the reaction indicate degradation of the Ru complex (Figure S33). Since the degradation of the Ru catalyst during the reaction was inevitable, we compared the catalytic efficiencies of the polymers in the early stage of the reaction. After 30 min, the linear polymer (**P4**) and **SCNP3-CL2** showed conversions of close to 16 and 18%, respectively (Table 2). These values exceed those observed for the free pyrene–$Ru(bpy)_3^{2+}$ system (12%), demonstrating that the polymer systems exhibit higher efficiencies than the free pyrene-$Ru(bpy)_3^{2+}$ system. Furthermore, the higher conversion of **SCNP3-CL2** compared to **P4** suggests that the compact polymer structure is advantageous for the intramolecular PET reaction. The previously determined quantum yields indicate an approximately tenfold difference in PET efficiency between the free photosensitizer and copolymer system. Although the observed difference in catalytic activity was less dramatic than that seen in SCNP formation – most likely because substrate diffusion into the SCNP becoming the rate limiting step – the effectiveness of macromolecular confinement is evident in the photocatalytic reaction.

Finally, the effects of SCNP compaction were quantitatively evaluated by comparing **SCNP3-CL7** and **SCNP3-CL11**. As the cross-linking ratio increased, a gradual decrease in reaction conversion was observed (Figure 5C), suggesting that increasing the cross-linking ratio does not result in a steady increase in reaction efficiency, which indicates the existence of a goldilocks confinement range for an optimal intramolecular PET reaction. Furthermore, this result dismisses the possibility that the higher initial conversion of **SCNP3-CL2** compared to the linear polymer (**P4**) is due to the presence of additional PyCh-dimer at the cross-linking points.

To assess the physical properties of these polymers, we compared their flexibility in solution using spin–spin (T_2) relaxation time measurement. The T_2 relaxation time reflects the decay of FID signals in NMR measurements, where a longer T_2 relaxation time indicates greater molec-

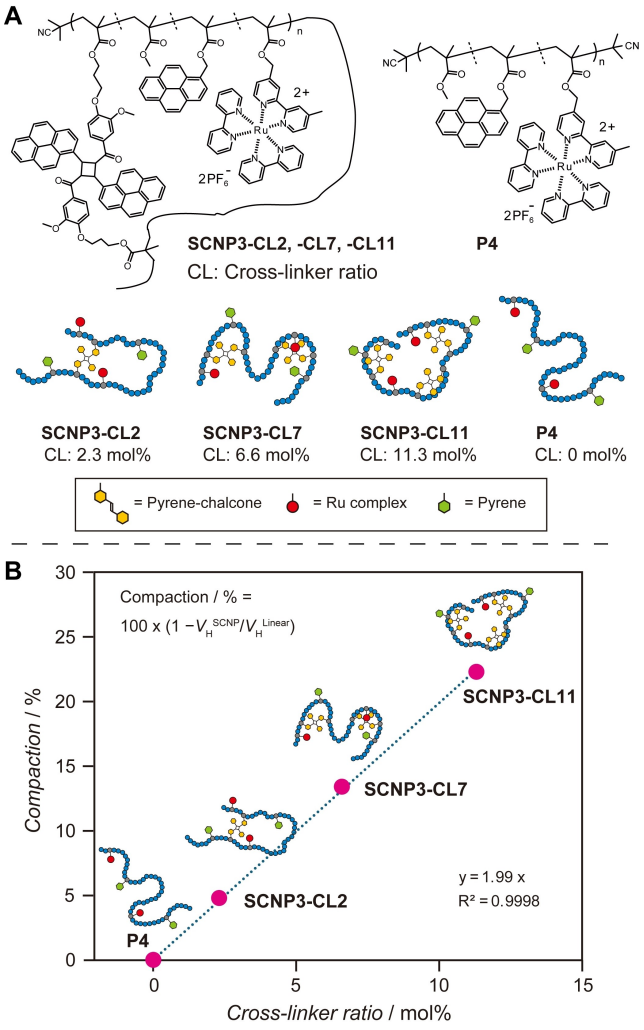

Figure 4. **(A)** Chemical structures of photocatalytic polymers (**SCNP3-CL2**, **-CL7**, **-CL11**, and **P4**) and their schematic illustrations. **(B)** Compaction percentage versus cross-linker ratio of the photocatalytic polymers.

ular mobility (flexibility), and vice versa.[12] The T_2 values measured at 0.87 ppm (PMMA-CH_3) in the ^{1}H NMR spectra are depicted in Figure 5D (Table S12 and Figure S34–S47). **SCNP3-CL2, -CL7**, and **-CL11** all exhibited shorter T_2 values than their linear precursors (**P3-CL2**, **-CL7**, **-CL11**), with the T_2 decrease, correlating with the cross-linking ratio. These data demonstrate that higher crosslinking ratios in SCNPs result in more rigid structures and that a certain level of flexibility in the polymer chains is required for efficient energy/electron transfer within a SCNP environment.[13] Our findings demonstrate that compact macromolecular entities can enhance catalytic function. We hypothesize that the decrease in the catalytic activity within too compact polymer structures is associated with the random nature of the copolymer structures. Higher degrees of crosslinking stiffen the polymer backbone thereby separating the photoactive units. Less crosslinked SCNPs are more flexible and have more degrees of freedom that allow the photoactive units to come in close contact. To achieve even superior functionality in SCNPs, future work must focus on strategies that allow to carefully tailor the precise molecular environment around the catalytic center, exploiting sequence control and locally ordered conformations.[2g,14]

Conclusion

We introduce reactive macromolecules for photoinduced energy/electron transfer (PET) system into single-chain nanoparticles (SCNPs) and demonstrate the effects of macromolecular confinement in two photoinduced reactions. The co-introduction of a Ru complex photosensitizer into a single-chain polymer accelerates the construction of SCNPs via PET-enhanced photocross-linking. Critically, the SCNPs exhibit superior photocatalytic performance compared to small molecule analogs and their linear polymer counterparts, attributed to the confinement of the catalytic moieties. Interestingly, increasing the cross-linking ratio in the SCNPs does not result in a contineous increase in reaction efficiency, rather suggesting a goldilocks zone of optimum catalytic performance. Our work demonstrates the advantages of PET reactions executed in compact single-chain polymers. Tuning the SCNP flexibility is a key step forward the design of functional (nano)materials for photochemical applications.

Acknowledgements

M.N. is grateful to the support by Kyushu University World-leading Researchers Training Program (QUEST). M.N. thanks Dr. J. Carroll and Dr. R. R. Hawker (both QUT) for experimental support. M.N. additionally expresses gratitude to the members of the Soft Matter Materials team in Brisbane for welcoming him, especially the researchers in Laboratory Bay 1. C.B.-K. is grateful for an Australian Research Council (ARC) Laureate Fellowship enabling his photochemical research program as well as continued key support from the Queensland University of Technology (QUT). The Central Analytical Research Facility (CARF) at QUT is gratefully acknowledged for access to analytical instrumentation, supported by QUT's research portfolio.

Conflict of Interest

The authors declare no conflict of interest.

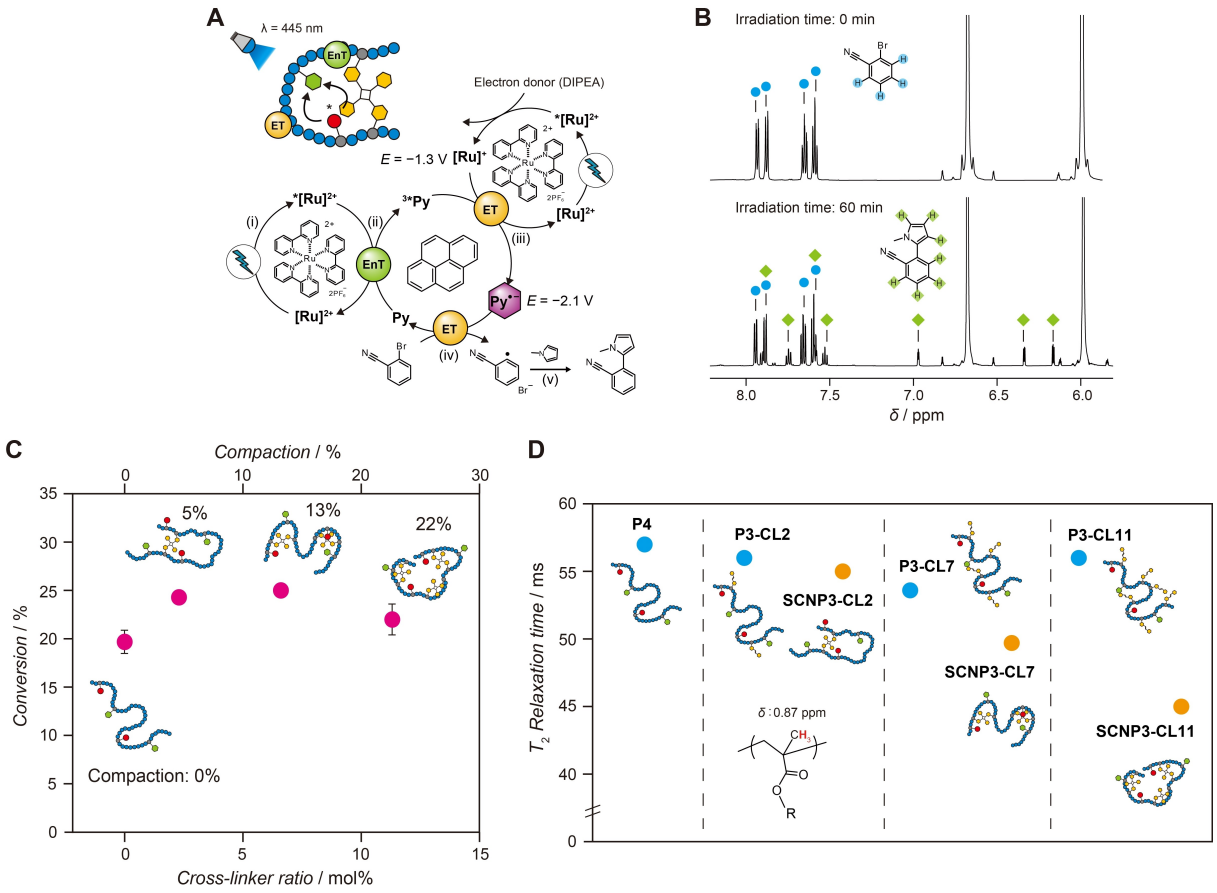

Figure 5. **(A)** Reaction mechanism of the photocatalytic reaction of the current study. **(B)** ^{1}H NMR spectra of reaction solution using **SCNP3-CL2** before and after LED irradiation (λ_{max} = 445 nm). Solvent was DMSO-d_6. Blue and green marks represent proton resonances assigned to 2-bromobenzonitrile (substrate) and 2-(1-methyl-1H-pyrrol-2-yl)benzonitrile (product). **(C)** Conversion of the photoredox reaction after irradiation for 60 min vs crosslinker ratio and compaction of each polymer catalyst. The experiments were triplicated. **(D)** T_2 relaxation time of the synthesized polymers at 0.87 ppm (methyl protons of main chain). Blue and yellow plots represent linear and SCNP polymers, respectively. The experiments were triplicated.

Data Availability Statement

The data that support the findings of this study are available from the corresponding author upon reasonable request.

Keywords: Photoinduced Energy Transfer · Polymers · Molecular Confinement · Single-Chain Nanoparticles (SCNPs) · Photoredox Reactions

[1] a) M. Ouchi, N. Badi, J.-F. Lutz, M. Sawamoto, *Nat. Chem.* **2011**, *3*, 917; b) J.-F. Lutz, J.-M. Lehn, E. W. Meijer, K. Matyjaszewski, *Nat. Rev. Mater.* **2016**, *1*, 16024; c) J.-F. Lutz, *ACS Macro Lett.* **2020**, *9*, 185; d) S. Wijker, A. R. A. Palmans, *ChemPlusChem* **2023**, *88*, e202300260; e) J. Xu, C. Fu, S. Shanmugam, C. J. Hawker, G. Moad, C. Boyer, *Angew. Chem. Int. Ed.* **2017**, *56*, 8376; f) J. M. Ren, J. Lawrence, A. S. Knight, A. Abdilla, R. B. Zerdan, A. E. Levi, B. Oschmann, W. R. Gutekunst, S.-H. Lee, Y. Li, A. J. McGrath, C. M. Bates, G. G. Qiao, C. J. Hawker, *J. Am. Chem. Soc.* **2018**, *140*, 1945; g) S. Perrier, *Macromolecules.* **2017**, *50*, 7433; h) Y. Saito, R. Honda, S. Akashi, H. Takimoto, M. Nagao, Y. Miura, Y. Hoshino, *Angew. Chem. Int. Ed.* **2022**, *61*, e202206456.

[2] a) J. A. Pomposo, I. Perez-Baena, F. Lo Verso, A. J. Moreno, A. Arbe, J. Colmenero, *ACS Macro Lett.* **2014**, *3*, 767; b) E. Verde-Sesto, A. Arbe, A. J. Moreno, D. Cangialosi, A. Alegría, J. Colmenero, J. A. Pomposo, *Mater. Horiz.* **2020**, *7*, 2292; c) O. Altintas, C. Barner-Kowollik, *Macromol. Rapid Commun.* **2012**, *33*, 958; d) R. Chen, E. B. Berda, *ACS Macro Lett.* **2020**, *9*, 1836; e) A. M. Hanlon, C. K. Lyon, E. B. Berda, *Macromolecules* **2016**, *49*, 2; f) C. K. Lyon, A. Prasher, A. M. Hanlon, B. T. Tuten, C. A. Tooley, P. G. Frank, E. B. Berda, *Polym. Chem.* **2015**, *6*, 181; g) J. L. Warren, P. A. Dykeman-Bermingham, A. S. Knight, *J. Am. Chem. Soc.* **2021**, *143*, 13228.

[3] a) H. Rothfuss, N. D. Knöfel, P. W. Roesky, C. Barner-Kowollik, *J. Am. Chem. Soc.* **2018**, *140*, 5875; b) J. Chen, E. S. Garcia, S. C. Zimmerman, *Acc. Chem. Res.* **2020**, *53*, 1244; c) T. Terashima, T. Mes, T. F. A. De Greef, M. A. J. Gillissen, P. Besenius, A. R. A. Palmans, E. W. Meijer, *J. Am. Chem. Soc.* **2011**, *133*, 4742; d) J. Chen, J. Wang, Y. Bai, K. Li, E. S. Garcia, A. L. Ferguson, S. C. Zimmerman, *J. Am. Chem. Soc.* **2018**, *140*, 13695; e) Y. Liu, S. Pujals, P. J. M. Stals, T. Paulöhrl, S. I. Presolski, E. W. Meijer, L. Albertazzi, A. R. A. Palmans, *J. Am. Chem. Soc.* **2018**, *140*, 3423; f) D. Arena, E. Verde-Sesto, I. Rivilla, J. A. Pomposo, *J. Am. Chem. Soc.* **2024**, *146*, 14397; g) F. Eisenreich, E. W. Meijer, A. R. A. Palmans, *Chem. Eur. J.* **2020**, *26*, 10355; h) M. A. Sanders, S. S. Chittari, N.

Sherman, J. R. Foley, A. S. Knight, *J. Am. Chem. Soc.* **2023**, *145*, 9686.

[4] a) K. Mundsinger, A. Izuagbe, B. T. Tuten, P. W. Roesky, C. Barner-Kowollik, *Angew. Chem. Int. Ed.* **2024**, *63*, e202311734; b) K. Mundsinger, B. T. Tuten, L. Wang, K. Neubauer, C. Kropf, M. L. O'Mara, C. Barner-Kowollik, *Angew. Chem. Int. Ed.* **2024**, *62*, e202302995.

[5] L. S. van Bezouwen, S. Caffarri, R. S. Kale, R. Kouřil, A.-M. W. Thunnissen, G. T. Oostergetel, E. J. Boekema, *Nat. Plants* **2017**, *3*, 17080.

[6] a) M. Spicuzza, S. P. Gaikwad, S. Huss, A. A. Lee, C. V. Craescu, A. Griggs, J. Joseph, M. Puthenpurayil, W. Lin, C. Matarazzo, S. Baldwin, V. Perez, D. A. Rodriguez-Acevedo, J. R. Swierk, E. Elacqua, *Polym. Chem.* **2024**, *15*, 1833; b) H. Shimakoshi, M. Nishi, A. Tanaka, K. Chikama, Y. Hisaeda, *Chem. Commun.* **2011**, *47*, 6548; c) J. Lee, W. J. Song, *J. Am. Chem. Soc.* **2023**, *145*, 5211; d) A. Tebo, A. Quaranta, V. L. Pecoraro, A. Aukauloo, *ChemPhotoChem* **2021**, *5*, 665; e) A. M. Bogdanov, A. Acharya, A. V. Titelmayer, A. V. Mamontova, K. B. Bravaya, A. B. Kolomeisky, K. A. Lukyanov, A. I. Krylov, *J. Am. Chem. Soc.* **2016**, *138*, 4807.

[7] a) H. Frisch, J. P. Menzel, F. R. Bloesser, D. E. Marschner, K. Mundsinger, C. Barner-Kowollik, *J. Am. Chem. Soc.* **2018**, *140*, 9551; b) P. H. Maag, F. Feist, H. Frisch, P. W. Roesky, C. Barner-Kowollik, *Chem. Sci.* **2024**, *15*, 5218; c) I. M. Irshadeen, V. X. Truong, H. Frisch, C. Barner-Kowollik, *Chem. Commun.* **2023**, *59*, 11959; d) S. Gillhuber, J. O. Holloway, K. Mundsinger, J. A. Kammerer, J. R. Harmer, H. Frisch, C. Barner-Kowollik, P. W. Roesky, *Chem. Sci.* **2024**, *15*, 15280; e) F. Pashley-Johnson, R. Munaweera, S. I. Hossain, S. C. Gauci, L. Delafresnaye, H. Frisch, M. L. O'Mara, F. E. Du Prez, C. Barner-Kowollik, *Nat. Commun.* **2024**, *15*, 6033.

[8] I. M. Irshadeen, K. De Bruycker, A. S. Micallef, S. L. Walden, H. Frisch, C. Barner-Kowollik, *Polym. Chem.* **2021**, *12*, 4903.

[9] a) B. Durham, J. V. Caspar, J. K. Nagle, T. J. Meyer, *J. Am. Chem. Soc.* **1982**, *104*, 4803; b) P. Dongare, B. D. B. Myron, L. Wang, D. W. Thompson, T. J. Meyer, *Coord. Chem. Rev.* **2017**, *345*, 86.

[10] a) I. Ghosh, R. S. Shaikh, B. König, *Angew. Chem. Int. Ed.* **2017**, *56*, 8544; b) M. Marchini, G. Bergamini, P. G. Cozzi, P. Ceroni, V. Balzani, *Angew. Chem. Int. Ed.* **2017**, *56*, 12820; c) I. Ghosh, J. I. Bardagi, B. König, *Angew. Chem. Int. Ed.* **2017**, *56*, 12822; d) M. S. Coles, G. Quach, J. E. Beves, E. G. Moore, *Angew. Chem. Int. Ed.* **2020**, *59*, 9522; e) F. Glaser, C. Kerzig, O. S. Wenger, *Chem. Sci.* **2021**, *12*, 9922.

[11] a) S. Huss, A. R. Walsh, A. Griggs, D. A. Rodriguez-Acevedo, D. M. Arias-Rotondo, E. Elacqua, *Polym. Chem.* **2023**, *14*, 4560; b) V. Balzani, P. Ceroni, A. Credi, M. Venturi, *Coord. Chem. Rev.* **2021**, *433*, 213758.

[12] a) F. Heatley, *Prog. NMR Spectrosc* **1979**, *13*, 47; b) L. F. Pinto, J. Correa, M. Martin-Pastor, R. Riguera, E. Fernandez-Megia, *J. Am. Chem. Soc.* **2013**, *135*, 1972.

[13] M. Nagao, Y. Miura, *ACS Macro Lett.* **2023**, *12*, 733.

[14] a) P. A. Dykeman-Bermingham, M. P. Bogen, S. S. Chittari, S. F. Grizzard, A. S. Knight, *J. Am. Chem. Soc.* **2024**, *146*, 8607; b) F. Sbordone, A. Micallef, H. Frisch, *Angew. Chem. Int. Ed.* **2024**, *136*, e202319839.